

stated already by Holian *et al.*, the transition pressures are in reasonably good agreement with experiment, so that the disagreement with experiment has to stem from the estimation of the transition temperature. Of the quantities needed to calculate T_{tr} , the transition entropy can be assumed to be known more reliably. The latent heat $(\Delta H)_{tr}$, on the other hand, is more susceptible to small errors in a number of ways. Such errors can arise from the use of incorrect interatomic potentials, the possible importance of three- and four-body interactions, crystal-field effects, and short-range correlations. An account of these various effects has been given by Niebel and Venables.¹⁴

We would like to thank Tom Reed and Tom Reilly for the able and cheerful way in which they provided technical support. One of the authors (J.P.F.) likes to thank the Physics Department and the Unidel Foundation for a very enjoyable stay at the University of Delaware.

This research was supported in part by National Science Foundation Grant No. DMR 78-01-307.

^(a)Permanent address: Department of Physics, Uni-

versity of Alberta, Edmonton, Alta. T6G 2J1, Canada.

¹C. Isenberg and C. Domb, in *Lattice Dynamics*, edited by R. F. Wallis (Pergamon, Oxford, 1965).

²W. G. Hoover, *J. Chem. Phys.* **49**, 1981 (1968).

³B. J. Alder, B. P. Carter, and D. A. Young, *Phys. Rev.* **183**, 831 (1969).

⁴B. L. Holian, W. D. Gwinn, A. C. Luntz, and B. J. Alder, *J. Chem. Phys.* **59**, 5444 (1973).

⁵J. P. Franck, *Phys. Rev. Lett.* **40**, 1272 (1978).

⁶J. P. Franck, *Chem. Phys. Lett.* **63**, 100 (1979).

⁷J. E. Vos, B. S. Blaisse, D. A. E. Boon, W. J. van Scherpenzeel, and R. Kingma, *Physica (Utrecht)* **37**, 51 (1967); J. E. Vos, R. V. Kingma, F. J. van der Gaag, and B. S. Blaisse, *Phys. Lett.* **24A**, 738 (1967).

⁸J. P. Franck, in *Proceedings of the International Conference on Martensitic Transformations*, Cambridge, Massachusetts, 1979 (to be published).

⁹Spectra-Physics, Mountain View, Cal.

¹⁰R. K. Crawford and W. B. Daniels, *J. Chem. Phys.* **55**, 5651 (1971).

¹¹I. L. Spain and S. Segall, *Cryogenics* **11**, 26 (1971).

¹²D. E. Beck, *Mol. Phys.* **14**, 311 (1968), and **15**, 332 (1968).

¹³R. L. Mills and A. F. Schuch, *J. Low Temp. Phys.* **16**, 305 (1974).

¹⁴K. F. Niebel and J. A. Venables, in *Rare Gas Solids*, edited by M. L. Klein and J. A. Venables (Academic, London, 1976), Vol. I.

Structure of Defect Cascades in Fast-Neutron-Irradiated Aluminum by Diffuse X-Ray Scattering

B. v. Guérard, D. Grasse, and J. Peisl

Sektion Physik, Universität München, 8 München 22, Germany

(Received 14 May 1979)

We measure diffuse x-ray scattering close to Bragg reflections in aluminum single crystals after irradiation with fast-reactor neutrons at 4.6 K. Detailed evaluation of the results for low irradiation dose demonstrates that defects are located in cascades (radius $r_K \approx 50$ Å; defect number, $Z_K \approx 200$). Within a cascade the defects form agglomerates ($r_A \approx 5$ Å, $Z_A \approx 3$). For irradiation doses $> 2.4 \times 10^{18}$ n/cm² the cascades partly overlap.

Irradiation of solids with fast heavy particles produces vacancies and interstitials (Frenkel pairs) in displacement cascades. The actual defect concentration and correlation within a cascade depend on the specific properties of the material and the irradiation conditions. Computer simulations¹⁻³ predict a cascade structure with a high-vacancy concentration (depleted zone) surrounded by a cloud of interstitials.⁴ A detailed understanding of the defect correlation in displacement cascades is of special interest as it strongly influences the formation of large defect agglomerates during thermal annealing after low-temperature irradiation or during irra-

diation at elevated temperatures. Thermally stable defect agglomerates are the central problem of reactor materials.

In this Letter we report measurements of the diffuse x-ray scattering close to Bragg reflections [Huang diffuse scattering (HDS)] from low-temperature neutron-irradiated Al crystals. This method has been used successfully to determine the symmetry and strength of point defects and to study the formation of defect clusters.⁵⁻⁸

We are able for the first time to detect a modification of the HDS close to the Bragg peak due to a nonrandom defect distribution. This gives detailed information on the defect distribution in

cascades and subcascades in neutron-irradiated Al. To our knowledge no other technique has been applied and would be capable to study the defect distribution in low-temperature neutron-irradiated solids. E.g., transmission electron microscopy can so far detect defects only after they have formed dense agglomerates of a minimum size of 20 Å.⁹

The HDS intensity distribution close to a Bragg peak is given by two Fourier transforms¹⁰⁻¹²

$$I_{\text{HDS}}(\vec{G}, \vec{q}) = |F|^2 \langle \bar{c}^2 \rangle |\vec{K} \cdot \vec{u}|^2 \sim |F|^2 \langle \bar{c}^2 \rangle \Pi K^2 / q^2. \quad (1)$$

$|F|$ is the scattering amplitude of the unit cell at measuring temperature, \bar{c} and \vec{u} are the Fourier spectra of the concentration fluctuations \bar{c} and the displacements \vec{u} of a single defect, respectively. \vec{K} is the scattering vector and $\vec{q} = \vec{K} - \vec{G}$ the distance to the next nearest reciprocal-lattice vector \vec{G} . It is determined by the symmetry and strength of the defects and known from literature.^{7, 13}

For a random defect distribution $\langle \bar{c}^2 \rangle = c(1 - c) \approx c$, where c is the defect concentration. For an arbitrary defect distribution

$$\langle |\bar{c}|^2 \rangle = c(1 - c) + \sum_{\rho} \epsilon(\vec{\rho}) e^{i\vec{q} \cdot \vec{\rho}}, \quad (2)$$

where $\epsilon(\rho)$ is the deviation of the pair correlation function from the random one. When a concentration, c , of defects exists in the form of agglomerates of Z defects, one gets

$$\langle |\bar{c}|^2 \rangle = Zc. \quad (3)$$

The HDS intensity increases by a factor of Z due to defect agglomeration. For a more general non-random defect distribution (e.g., defects restricted to certain volumes only) it depends on the distance from the Bragg peak \vec{q} whether one observes scattering from the single defects or from the correlated defects.

The special case where Z_K defects are restricted to a spherical volume with radius r_K shows all the essential features. For small values of q , the scattering intensity will be increased by a factor Z_K whereas for large values of q , the scattering intensity becomes equal to what one expects from an uncorrelated random distribution. Because of the Fourier transformation in Eq. (2) a discontinuous defect distribution causes oscillations for $qr_K \gtrsim 4$.

The simple relation given in Eq. (1) is only valid as long as $|\vec{u} \cdot \vec{K}| < 1$. Close to defect clusters the lattice distortions can be so large that

$|\vec{u} \cdot \vec{K}| \geq 1$. In this case a different type of scattering is observed.¹¹ The asymptotic scattering is

$$I_{\text{AS}} \sim c |K| / q^4. \quad (4)$$

The change from $1/q^2$ dependence to $1/q^4$ dependence occurs at a certain value of \vec{q} related to $|\vec{u} \cdot \vec{K}| \approx 1$ and gives a distance R_{c1} at which the lattice distortions change the phase of the scattered wave drastically.

The experimental setup and procedure will be described in detail elsewhere. Here only some essential aspects will be given. The intensity distribution of scattered Cu $K\alpha_1$ radiation having passed a bent quartz monochromator was measured point by point for various settings of crystal and detector angle. The resolution volume in reciprocal space was optimized¹⁴ and had a size 9×10^7 times the volume of the Brillouin zone. The incoming intensity from a stabilized 6-kW generator (rotating anode, Rigaku) was monitored by a second counter. The scattered intensity was put on an absolute scale in the usual way by scattering from polystyrene.¹⁵ The defect-induced diffuse scattered intensity was obtained as the difference between scattered intensity from the crystals after irradiation and after complete thermal annealing. Pure Al single crystals (99.999% purity) were used, oriented in the appropriate way. The crystals were irradiated in the low-temperature irradiation facility of the Munich Research Reactor FRM at 4.6 K. After irradiation the crystals were transferred without raising the temperature to a special liquid-helium cryostat for the x-ray measurements. The measurements were performed at 8 K. During the whole procedure (irradiation, transfer, annealing, and measurements) the electrical resistivity of a wire sample treated in the same way was measured for comparison. (Some resistivity data are given in Table I.)

Scattering measurements for various irradiation doses were performed on crystals of different orientations giving results for different points \vec{G} and directions \vec{q} in the reciprocal lattice. Figure 1 shows a typical result. The scattered intensity close to a (400) Bragg reflection measured in [100] direction is given for an Al crystal after irradiation with 1×10^{18} n/cm² (circles) and after thermal annealing (crosses). The scattering distributions in Fig. 1 have been shifted to make the positions of the Bragg peaks, which are shifted because of the lattice parameter change $\Delta a/a$, coincide. The pronounced asymmetry of the defect-induced scattering intensity about the

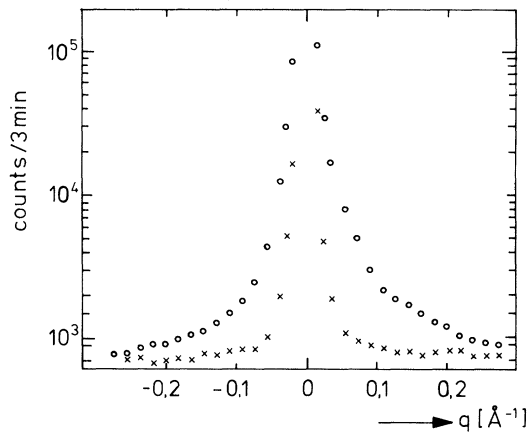


FIG. 1. Diffuse scattered x-ray intensity from Al single crystal near (400) reflection in [100] direction. Circles, after irradiation at 4.6°K with 1×10^{18} n/cm²; crosses, after thermal annealing at 200°C.

Bragg peak indicates that the distortion field in the irradiated crystal is dominated by defects which expand the lattice, i.e., interstitials.¹¹ The averaged intensity from both sides is plotted in Fig. 2 on a double logarithmic scale versus q (open circles). The typical q^{-2} and q^{-4} dependence is clearly demonstrated. For comparison the HDS intensity to be observed for the same defect concentration after electron irradiation is also shown in Fig. 2 (dash-dotted line). The increase of the scattered intensity by a factor of about 3 in neutron-irradiated crystals is due to defect correlations in small agglomerates. A further increase can be detected very close to the Bragg peak. This is demonstrated more clearly in Fig. 3, where the intensity is plotted after multiplication by q^2 in order to compensate the q^{-2} decrease. Results for three neutron doses are shown, in which the different reflections are scaled (division by $|F^2|/|PK^2|$) so that the relative intensities depend only on $\langle \tilde{c}^2 \rangle$. For low dose, the intensity increases for small q and shows the oscillations discussed earlier. With increasing neutron dose the increase at low q is less pronounced and the period of the oscillations changes. The solid lines have been calculated from Eq. (2) with the assumption that the cascades are spherical with a radius $r_K = 50$ Å. For the high-dose curves, correlation effects between cascades were taken into account.¹⁶ The radius of the spherical cascade volume was determined to be $r_K = (50 \pm 5)$ Å from a best fit to the experimental data.

From the average intensity at large q , we conclude [Eq. (3)] that interstitials¹⁷ are not randomly

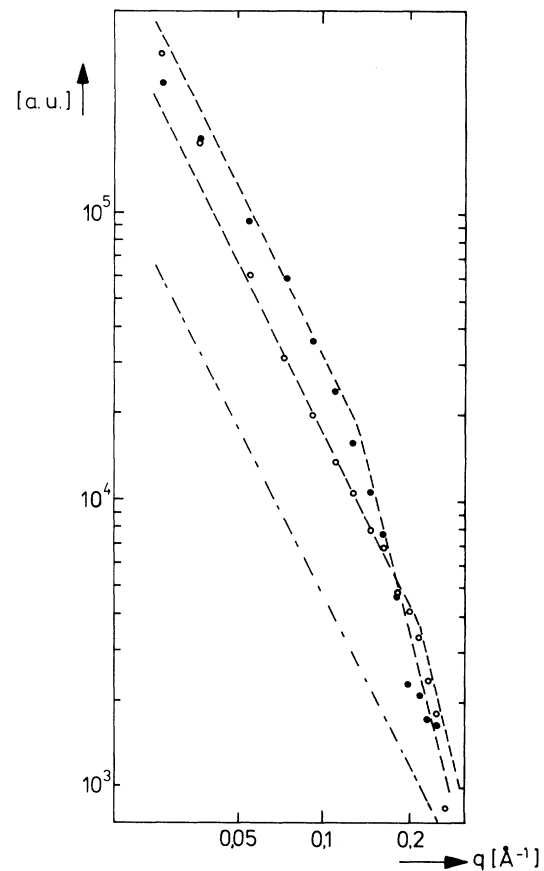


FIG. 2. Defect-induced scattering intensity from Al near (400) in [100] direction. Open circles, after irradiation at 4.6 K with 1×10^{18} n/cm²; closed circles, after thermal annealing at 70 K; dash-dotted line, expected intensity for the same defect concentration caused by electron irradiation.

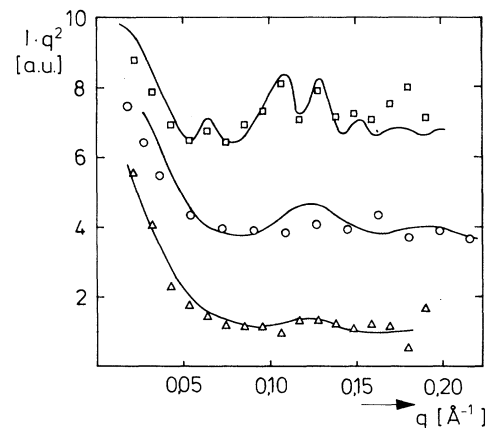


FIG. 3. Huang diffuse scattering intensity from neutron-irradiated Al. The solid lines are calculated from Eq. (2). The plotted points are identified in Table I.

TABLE I. Dose, geometry, resistivity, and c for data shown in Fig. 3.

Symbol	Neutron dose (10^{18} n/cm $^{-2}$)	\vec{G}	\vec{q}	$\Delta \rho$ (n Ω cm)	c
Δ	0.5	(222)	[111]	127	0.32×10^{-3}
\circ	1	(400)	[100]	314	0.8×10^{-3}
\square	2.4	(222)	[111]	446	1.13×10^{-3}

distributed in the cascade but form small agglomerates with a number of $Z=3$ (see also Fig. 2). Figure 3 also shows for these q that the scattering intensity increases proportional to the single-defect concentration. This means that the average number of interstitials in the small agglomerates is essentially independent of irradiation dose up to 2.4×10^{18} n/cm 2 . From that q^{-2} in Fig. 2 where the q^2 dependence goes to the q^{-4} dependence we can estimate a radius $r_A \approx 5$ Å for the highly distorted region around the small agglomerates of three interstitials. Together with the defect concentration from electrical resistivity, an estimate of the number of primary knock-on high-energy atoms yields a number of $Z_K \approx 200$ defects, with about 70 agglomerates in a main cascade. (In the evaluations it was assumed that the resistivity of the defects add linearly when they form small agglomerates or lie together in loose clusters like in a cascade.)¹⁸ The number of defects in a cascade could be determined directly from HDS if the resolution were high enough to measure even closer to the Bragg peaks. This could also tell whether the main cascades are split into several subcascades. In this case the radius $r_K = 50$ Å determined above would belong to such a subcascade.

The formation of displacement cascades and subcascades was predicted theoretically.³ There is no evidence from these computer calculations for the formation of small interstitial agglomerates as observed here. It has been proposed¹⁹ that interstitial clustering occurs subsequent to the dynamic production (which lasts 10^{-13} sec) of a cascade.

During thermal annealing the size of the agglomerates grows as soon as interstitials become mobile (state I). This can be seen in Fig. 2 from the diffuse intensity after annealing the sample to 70 K. At this temperature only 55% of the original defect concentration, as determined from the resistivity change, remains in the crystal. In spite of this, the HDS intensity increases because of clustering of the remaining defects.

The authors acknowledge the support by Dr. K. Bönig and his group with the low-temperature reactor irradiation. This work supported by the Bundesministerium für Forschung und Technologie.

¹J. B. Gibson, A. N. Goland, M. Milgram, and G. H. Vineyard, Phys. Rev. **120**, 1229 (1960).

²M. T. Robinson and I. M. Torrens, Phys. Rev. B **9**, 5008 (1974).

³J. R. Beeler, Jr., Phys. Rev. **150**, 470 (1966).

⁴L. A. Beavan, R. M. Scanlan, and D. N. Seidman, Acta Metall. **19**, 1339 (1971).

⁵H. Lohstöter, H. Spalt, and H. Peisl, Phys. Rev. Lett. **29**, 224 (1972).

⁶H. Spalt, H. Lohstöter, and H. Peisl, Phys. Status Solidi B **56**, 469 (1973).

⁷P. Erhard and W. Schilling, Phys. Rev. B **8**, 2604 (1973).

⁸B. von Guérard and H. Peisl, in *Fundamental Aspects of Radiation Damage in Metals*, edited by M. T. Robinson and F. W. Young, Jr., Conf.-751006 (Oak Ridge National Laboratory, Oak Ridge, Tenn., 1975), Vol. 1.

⁹B. L. Eyre, J. Phys. F **3**, 422 (1973).

¹⁰M. A. Krivoglaz, *Theory of X-Ray and Thermal Neutron Scattering by Real Crystals* (Plenum, New York, 1969).

¹¹P. H. Dederichs, J. Phys. F **3**, 471 (1973).

¹²H. Trinkaus, Phys. Status Solidi B **51**, 307 (1972).

¹³H.-G. Haubold, in *Fundamental Aspects of Radiation Damage in Metals*, edited by M. T. Robinson and F. W. Young, Jr., Conf.-751006 (Oak Ridge National Laboratory, Oak Ridge, Tenn., 1975), Vol. 1.

¹⁴H. Peisl, Acta Crystallogr. **8**, 143 (1975).

¹⁵C. J. Sparks and B. Borie, in *Local Atomic Arrangements Studied by X-Ray Diffraction*, Metallurgy Society Conference No. 36 (Gordon and Breach, New York, 1966).

¹⁶P. Debye, Phys. Z. **28**, 135 (1927).

¹⁷II differs for interstitials and vacancies in Al by a factor of 100 due to the difference in the relative volume change. Therefore the scattering is completely due to interstitials.

¹⁸W. Hertz and H. Peisl, J. Phys. F **5**, 2241 (1975).

¹⁹Yu. V. Martynenko, Radiat. Eff. **29**, 129 (1976).